

Q-boson interferometry and generalized Wigner function

Q. H. Zhang^a and Sandra S. Padula^b

Physics Department, McGill University, Montreal H3A 2T8, Canada

Instituto de Física Teórica, Rua Pamplona 145, 01405-900 São Paulo, Brazil

Bose-Einstein correlations of two identically charged Q -bosons are derived when these particles, are confined in finite volumes. Boundary effects on single Q -boson spectrum are also studied. We derive a generalized form for the Wigner function depending on the deformation parameter Q , which reduces to the original functional form in the limit of $Q \rightarrow 1$.

I. INTRODUCTION

Two-boson interferometry has for a long time been linked to high energy heavy-ion collisions as one of the tools to probe the existence of a new phase of matter of strongly interaction particles, the quark-gluon plasma (QGP), at high temperature and high baryon density [1,2]. The hope of discovering the QGP in high energy heavy-ion collisions is to some extent connected to the possibility of measuring the geometrical sizes of the emission region of secondary particles. And that is the connection point, i.e., so-called Hanbury-Brown-Twiss (HBT) interferometry [3,4] method, originally proposed in the 50's for measuring stellar radii. This method has been largely studied over the last twenty years, and has extensively been developed and improved ever since [5].

In a previous paper [6], we have studied boundary effects on the single-particle distribution and on the two-particle correlation function, motivated by the need to consider more realistic finite systems and by the idea suggested in Ref. [7]. In this reference it was shown in that in heavy-ion collisions, the pion system could be thought as a liquid of quasipions subjected to a surface tension. Naturally, it would be expected that this surface tension would affect the spectrum distribution, which was shown in Ref. [6,8,9,10,11,12]. As pion interferometry is sensitive to the geometrical size of the emission region as well as to the underlying dynamics, we would expect that the boundary would also affect the correlation function, which was indeed demonstrated in Ref. [6].

On the other hand, a Q -boson concept was suggested [13] some time ago associated to a *deformation parameter*, Q , which was viewed as an effective parameter able to encapsulate many essential features of complex dynamics of different systems. (We call the attention to the notation adopted here. We use Q to refer to the bosons

under study here for avoiding confusion with the relative momentum of the bosonic pairs, $q = k_1 - k_2$, commonly used in interferometry and maintained here as well). Effectively, the way it works is by reducing the complexity of the interacting systems under study into simpler relations, nevertheless paying the price of deforming, and thus complicating, the commutation relations of those systems. These are known as the Q -deformed algebras, a approach which have been widely studied in statistical physics [14] and also in heavy-ion collisions physics in Ref. [15]. Particularly interesting is the approach in Ref. [16], where it was shown that the composite nature of the particles (pseudoscalar mesons) under study could result into Q -deformed structures linked to the deformation parameter Q . In that reference is then interpreted as a means to measure the effects of the internal degrees of freedom of the composite particles (mesons, in our case), the value of Q depending on the *degree of overlap* of the extended structure of the particles in the medium. In this approach, the Q -parameter could then be related to the power of "probing lenses" for mimicking the effects of internal constituents of the bosons. Being so, if this power was high enough, it would mean that the bosonic behavior of the Q -bosons would be blurred by the fermionic effect of their internal constituents, which would result in decreasing the value of Q . We will see that our results are compatible with this interpretation.

In any case, independently of the interpretation given to the Q -bosons, and recalling the sensitivity of interferometry to the underlying dynamics of the system under study, it would be interesting to analyse its effects on the two identical Q -bosons correlation function. Besides, adding this extra degree of freedom extends and generalizes our previous approach.

In view of our previous study of confined pions subjected to finite size boundaries, and to the Q -boson approach mentioned above, Ref. [15] turned to be of special interest to our investigation. However, in that reference, only the so-called *coherent or chaoticity parameter*, λ , i.e., the intercept of two-particle correlation function at zero momentum difference, (i.e., $C(q = 0, K) - 1$), was studied and restricted only to single modes. All the possible effects on the effective geometrical information, which is actually of more interest to physics, were completely neglected. Besides, many other well-known sources of effects can contribute to yield values of λ smaller than the unity. In this paper we will develop a full Q -boson two-particle interferometric relation and simultaneously study the extra effect that the finite size boundary could

have on the Q -boson spectrum and on Q -boson interferometry.

The plan of this paper is the following: in section II, we derive the Q -boson single-inclusive distribution, as well as the two- Q -boson correlation function, considering a density matrix suited for describing charged identical Q -boson correlation effects. In section III, the boundary effects on the two- Q -boson correlation and single particle spectrum distribution are illustrated by means of two simple specific examples. Finally, conclusions are discussed in section IV.

II. SPECTRUM AND TWO- Q -BOSON CORRELATION FUNCTION

In this section, we derive a general relation for describing the single- as well as for the two-particle inclusive distributions, which would be suited for describing charged Q -bosons bounded in a finite volume. For doing this, we extend the hypotheses assumed in Ref. [6] to the pions considered here as a Q -boson system. Essentially, these could be summarized as follows: the effects of interaction among the Q -bosons could be modeled by considering that they move in an attractive mean field potential, which extends over the whole system. In the two-(quasi)particle case, this implies that they would not suffer any other effects besides the mean field attraction and the identical particle symmetrization. The effect due to the fermionic (constituents) internal degrees of freedom, along the lines suggested in Ref. [16], if any, would be represented by the effective deformation parameter Q . Also in the present analysis, as we assumed before [6], we consider that the pions represented by Q -bosons to be quasi-bound in the system, with the surface tension [7] acting as a reflecting boundary. This could, for instance, mimic a stage immediately before the freeze-out of the (decoupling) system, when confinement of the quarks and gluons is already in effect. The Q -boson wave function could then be considered as vanishing outside this boundary. Once more, we assume that these particles become free when their average separation is larger than their interaction range and we consider this transition to happen very rapidly, in such a way that the momentum distribution of the Q -bosons could be essentially governed by their momentum distribution just before they freeze out. We then study the modifications on the observed Q -boson momentum distribution caused by the presence of this boundary. On the other hand, we know that interferometry is sensitive to the geometrical size of the emission region as well as to the underlying dynamics, and, we would expect that the boundary would also affect the correlation function, similarly as it affected the pions in [6]. However, as we shall see later, there is a significant difference in the present case: the parameter

named long time ago as *chaoticity* or *coherence*, λ , will be considerably different as compared to the case of a normal (i.e., in the limit of $Q \rightarrow 1$) pion, but will be recovered in the appropriate limit.

For deriving the relations that allow to describe the single- and two-particle inclusive distributions, we start by assuming that the Q -boson creation operator in coordinate space can be expressed by [15]

$$\hat{\psi}^\dagger(\mathbf{x}) = \sum_l \hat{a}_l^\dagger \psi_l^*(\mathbf{x}), \quad (1)$$

where \hat{a}_l^\dagger is the creation operator for creating a Q -boson in a quantum state characterized by a quantum number l . Then, $\psi_l(\mathbf{x})$ is one of eigenfunctions belonging to a localized complete set, which satisfies the orthonormality condition

$$\int d\mathbf{x} \psi_l^*(\mathbf{x}) \psi_{l'}(\mathbf{x}) = \delta_{l,l'}, \quad (2)$$

and completeness relation

$$\sum_l \psi_l^*(\mathbf{x}) \psi_l(\mathbf{y}) = \delta(\mathbf{x} - \mathbf{y}). \quad (3)$$

Similarly, the Q -boson annihilation operator in coordinate space can be written as

$$\hat{\psi}(\mathbf{x}) = \sum_l \hat{a}_l \psi_l(\mathbf{x}). \quad (4)$$

In momentum space, the corresponding Q -boson creation operator, $\hat{\psi}^\dagger(\mathbf{p})$, and annihilation operator, $\hat{\psi}(\mathbf{p})$, can be expressed, respectively, as

$$\hat{\psi}^\dagger(\mathbf{p}) = \sum_l \hat{a}_l^\dagger \tilde{\psi}_l^*(\mathbf{p}) \quad (5)$$

and

$$\hat{\psi}(\mathbf{p}) = \sum_l \hat{a}_l \tilde{\psi}_l(\mathbf{p}), \quad (6)$$

where

$$\tilde{\psi}_l(\mathbf{p}) = \frac{1}{(2\pi)^{3/2}} \int \psi_l(\mathbf{x}) e^{i\mathbf{p}\cdot\mathbf{x}} d\mathbf{x}. \quad (7)$$

The Q -bosons are then defined by means of the algebra satisfied by their creation and annihilation operators, i.e., [15]

$$\begin{aligned} a_l a_{l'}^\dagger - Q^{\delta_{l,l'}} a_{l'}^\dagger a_l &= \delta_{l,l'} \\ [a_l, a_{l'}] &= [a_l^\dagger, a_{l'}^\dagger] = 0, \\ [\hat{N}_l, a_{l'}] &= -\delta_{l,l'} a_l \\ [\hat{N}_l, a_{l'}^\dagger] &= \delta_{l,l'} a_l^\dagger, \\ [\hat{N}_l, \hat{N}_{l'}] &= 0, \end{aligned} \quad (8)$$

Here Q is a (C-number) parameter, which is assumed to be within the interval $[-1, 1]$, and \hat{N}_l is the number operator, which can be expressed as

$$\hat{N}_l = \sum_{s=1}^{\infty} \frac{(1-Q)^s}{(1-Q^s)} (a_l^\dagger)^s (a_l)^s. \quad (9)$$

It can be easily verified that, for $Q = 1$, the normal bosonic limit is recovered, i.e., the particles then obey the regular bosonic commutation relations, as it would be expected.

We write the density matrix operator for our Q -bosonic system as

$$\begin{aligned} \hat{\rho} &= \exp \left[-\frac{1}{T} (\hat{H} - \mu \hat{N}) \right] = \prod_l \rho_l, \\ \rho_l &= \exp \left[-\frac{1}{T} (\hat{H}_l - \mu \hat{N}_l) \right], \end{aligned} \quad (10)$$

where

$$\hat{H} = \sum_l \hat{H}_l; \quad \hat{H}_l = E_l \hat{N}_l; \quad \hat{N} = \sum_l \hat{N}_l, \quad (11)$$

are the Hamiltonian and number operators, respectively; T is the temperature.

The corresponding normalization is explicitly included in the definition of the expectation value of observables as, for instance, for an operator \hat{A}

$$\langle \hat{A} \rangle = \frac{\text{tr}\{\hat{\rho}\hat{A}\}}{\text{tr}\{\hat{\rho}\}}. \quad (12)$$

With the above definitions, it is easy to verify that

$$\text{tr}(\rho_l) = \sum_n \langle n | \rho_l | n \rangle_l = \frac{1}{1 - \exp[-\frac{1}{T}(E_l - \mu)]}, \quad (13)$$

where

$$|n\rangle_l = \frac{1}{\sqrt{[n]!}} (a_l^\dagger)^n |0\rangle; \quad [n] = \frac{1 - Q^n}{1 - Q}. \quad (14)$$

From the above equations, we can compute the expectation values

$$\langle a_l^\dagger a_l \rangle = \frac{1}{\exp[\frac{1}{T}(E_l - \mu)] - Q}, \quad (15)$$

and

$$\langle a_l^\dagger a_l^\dagger a_l a_l \rangle = \frac{1+Q}{\{e^{\frac{1}{T}(E_l - \mu)} - Q\} \{e^{\frac{1}{T}(E_l - \mu)} - Q^2\}}. \quad (16)$$

Then, the single Q -boson distribution can be written as

$$\begin{aligned} P_1(\mathbf{p}) &= \langle \hat{\psi}^\dagger(\mathbf{p}) \hat{\psi}(\mathbf{p}) \rangle \\ &= \sum_l \sum_{l'} \tilde{\psi}_l^*(\mathbf{p}) \tilde{\psi}_{l'}(\mathbf{p}) \langle a_l^\dagger a_{l'} \rangle. \end{aligned} \quad (17)$$

The expectation value $\langle \hat{a}_l^\dagger \hat{a}_{l'} \rangle$ is related to the occupation probability of a single-particle state l , N_l , by the following relation

$$\langle \hat{a}_l^\dagger \hat{a}_{l'} \rangle = \delta_{l,l'} N_l. \quad (18)$$

For a Q -bosonic system in equilibrium at a temperature T and chemical potential μ , N_l is represented by the modified Bose-Einstein distribution

$$N_l = \frac{1}{\exp[\frac{1}{T}(E_l - \mu)] - Q}. \quad (19)$$

By inserting Eq. (18) and (19) into (17), we obtain the single-particle spectrum for one Q -boson species as

$$P_1(\mathbf{p}) = \sum_l N_l \tilde{\psi}_l^*(\mathbf{p}) \tilde{\psi}_l(\mathbf{p}). \quad (20)$$

Similarly, the two- Q -boson distribution function can be written as

$$\begin{aligned} P_2(\mathbf{p}_1, \mathbf{p}_2) &= \langle \hat{\psi}^\dagger(\mathbf{p}_1) \hat{\psi}^\dagger(\mathbf{p}_2) \hat{\psi}(\mathbf{p}_1) \hat{\psi}(\mathbf{p}_2) \rangle \\ &= \sum_{l_1, l_2, l_3, l_4} \tilde{\psi}_{l_1}^*(\mathbf{p}_1) \tilde{\psi}_{l_2}^*(\mathbf{p}_2) \tilde{\psi}_{l_3}(\mathbf{p}_1) \tilde{\psi}_{l_4}(\mathbf{p}_2) \\ &\quad \langle \hat{a}_{l_1}^\dagger \hat{a}_{l_2}^\dagger \hat{a}_{l_3} \hat{a}_{l_4} \rangle \\ &= \sum_{l_1, l_2, l_3, l_4} \tilde{\psi}_{l_1}^*(\mathbf{p}_1) \tilde{\psi}_{l_2}^*(\mathbf{p}_2) \tilde{\psi}_{l_3}(\mathbf{p}_1) \tilde{\psi}_{l_4}(\mathbf{p}_2) \\ &\quad \left[\langle \hat{a}_{l_1}^\dagger \hat{a}_{l_3} \rangle \langle \hat{a}_{l_2}^\dagger \hat{a}_{l_4} \rangle_{l_1 \neq l_2} \right. \\ &\quad + \langle \hat{a}_{l_1}^\dagger \hat{a}_{l_4} \rangle \langle \hat{a}_{l_2}^\dagger \hat{a}_{l_3} \rangle_{l_1 \neq l_2} \\ &\quad \left. + \langle \hat{a}_{l_1}^\dagger \hat{a}_{l_2}^\dagger \hat{a}_{l_3} \hat{a}_{l_4} \rangle_{l_1=l_2=l_3=l_4} \right] \\ &= P_1(\mathbf{p}_1) P_1(\mathbf{p}_2) + \left| \sum_l N_l \tilde{\psi}_l^*(\mathbf{p}_1) \tilde{\psi}_l(\mathbf{p}_2) \right|^2 \\ &\quad + \sum_l \tilde{\psi}_l^*(\mathbf{p}_1) \tilde{\psi}_l^*(\mathbf{p}_2) \tilde{\psi}_l(\mathbf{p}_1) \tilde{\psi}_l(\mathbf{p}_2) \times \\ &\quad \left[\langle \hat{a}_l^\dagger \hat{a}_l^\dagger \hat{a}_l \hat{a}_l \rangle - 2 \langle \hat{a}_l^\dagger \hat{a}_l \rangle^2 \right] \end{aligned} \quad (21)$$

Using Eq.(14,15), we finally have

$$\begin{aligned} P_2(\mathbf{p}_1, \mathbf{p}_2) &= P_1(\mathbf{p}_1) P_1(\mathbf{p}_2) + \left| \sum_l N_l \tilde{\psi}_l^*(\mathbf{p}_1) \tilde{\psi}_l(\mathbf{p}_2) \right|^2 \\ &\quad - \sum_l \tilde{\psi}_l^*(\mathbf{p}_1) \tilde{\psi}_l^*(\mathbf{p}_2) \tilde{\psi}_l(\mathbf{p}_1) \tilde{\psi}_l(\mathbf{p}_2) \times \\ &\quad (1 - Q) \cdot N_l^2 \frac{\exp[\frac{1}{T}(E_l - \mu)] + Q}{\exp[\frac{1}{T}(E_l - \mu)] - Q^2} \end{aligned} \quad (22)$$

The two-particlecorrelation can then be written as

$$\begin{aligned} C_2(\mathbf{p}_1, \mathbf{p}_2) &= \frac{P_2(\mathbf{p}_1, \mathbf{p}_2)}{P_1(\mathbf{p}_1) P_1(\mathbf{p}_2)} = \\ &= 1 + \left\{ \sum_l N_l |\tilde{\psi}_l(\mathbf{p}_1)|^2 \sum_l N_l |\tilde{\psi}_l(\mathbf{p}_2)|^2 \right\}^{-1} \times \end{aligned}$$

$$\sum_{l,l'} N_l N_{l'} \tilde{\psi}_l^*(\mathbf{p}_1) \tilde{\psi}_{l'}^*(\mathbf{p}_2) \tilde{\psi}_l(\mathbf{p}_2) \tilde{\psi}_{l'}(\mathbf{p}_1) \times \left\{ 1 - \delta_{l,l'} (1 - Q) \cdot \frac{\exp(\frac{1}{T}(E_l - \mu)) + Q}{\exp(\frac{1}{T}(E_l - \mu)) - Q^2} \right\} . \quad (23)$$

It is interesting to note that, for $Q=1$, we regain the results in Ref [6]. Moreover, for $Q=0$, we get identical results as shown in the **Appendix A** of that reference, corresponding to *classical* Boltzmann distribution.

From Eq. (23), it is straightforward to show that, when $\mathbf{q} = \mathbf{p}_1 - \mathbf{p}_2 = 0$,

$$C_2(\mathbf{p}, \mathbf{p}) = 2 - \frac{1}{\sum_l N_l |\tilde{\psi}_l(\mathbf{p})|^2 \sum_l N_l |\tilde{\psi}_l(\mathbf{p})|^2} \times [(1 - Q) \sum_l \tilde{\psi}_l^*(\mathbf{p}) \tilde{\psi}_l^*(\mathbf{p}) \tilde{\psi}_l(\mathbf{p}) \tilde{\psi}_l(\mathbf{p}) \cdot N_l^2 \times \frac{\exp(\frac{1}{T}(E_l - \mu)) + Q}{\exp(\frac{1}{T}(E_l - \mu)) - Q^2}] . \quad (24)$$

We see that, for $Q = 1$, we regain the ideal result for the bosonic intercept at the zero momentum difference, $\mathbf{q} = \mathbf{p}_1 - \mathbf{p}_2 = 0$, i.e., $C_2(\mathbf{p}, \mathbf{p}) = 2$. On the other hand, for $Q = 0$, we recover the expected Boltzmann result, $C_2(\mathbf{p}, \mathbf{p}) = 1$, which we can demonstrate by using the orthogonality and completeness conditions of the states.

From Eq.(24) the intercept of the correlation function, λ , usually known as the *coherence* or *chaoticity* parameter, can be immediately identified as

$$\lambda(k) = C_2(k, k) - 1 = 1 - \frac{(1 - Q)}{\sum_l N_l |\tilde{\psi}_l(\mathbf{k})|^2 \sum_l N_l |\tilde{\psi}_l(\mathbf{k})|^2} \times [\sum_l \tilde{\psi}_l^*(\mathbf{k}) \tilde{\psi}_l^*(\mathbf{k}) \times \tilde{\psi}_l(\mathbf{k}) \tilde{\psi}_l(\mathbf{k}) \cdot N_l^2 \left(\frac{\exp(\frac{1}{T}(E_l - \mu)) + Q}{\exp(\frac{1}{T}(E_l - \mu)) - Q^2} \right)] . \quad (25)$$

We see that the intercept decreases with decreasing Q , being always smaller than unity for $0 \leq Q \leq 1$. On the other hand, it is interesting to point that the definition for the chaoticity parameter given by Eq. (25) differs from the one in Ref. [15,17], mainly, but not only, because it is there defined exclusively for a single mode. In any case, although this is a delicate association, we could compare to the experimental points for λ , which has always been in the limit $0 \leq \lambda \leq 1$, as suggested in Ref. [15,17]. Nevertheless, we prefer not to do so because of it is well-known that other factors, such as resonances, dynamical and multiparticle effects, as well as kinematical cuts, could also cause the intercept to drop into that interval. The subtlety of the comparison is due to the fact that we know that resonances, dynamical and multiparticle effects, as well as kinematical cuts, could also cause the intercept to drop into that interval.

The above derivation can also be reformulated within the Wigner function approach. For doing this, we develop the product of four wave-functions $\psi^{(*)}$ in Eq. (23) into the product of the corresponding Fourier transforms, leading to

$$\begin{aligned} & \tilde{\psi}_l(\mathbf{p}_1) \tilde{\psi}_{l'}^*(\mathbf{p}_2) \tilde{\psi}_l(\mathbf{p}_2) \tilde{\psi}_{l'}(\mathbf{p}_1) = \\ & = \tilde{\psi}_l^*(\mathbf{p}_1) \tilde{\psi}_l(\mathbf{p}_2) \tilde{\psi}_{l'}^*(\mathbf{p}_2) \tilde{\psi}_{l'}(\mathbf{p}_1) \\ & = \int \frac{d^3 r_1}{(2\pi)^{3/2}} e^{-i\mathbf{p}_1 \cdot \mathbf{r}_1} \tilde{\psi}_l^*(\mathbf{r}_1) \int \frac{d^3 r_2}{(2\pi)^{3/2}} e^{i\mathbf{p}_2 \cdot \mathbf{r}_2} \psi_l(\mathbf{r}_2) \times \\ & \quad \int \frac{d^3 r'_2}{(2\pi)^{3/2}} e^{-i\mathbf{p}_2 \cdot \mathbf{r}'_2} \psi_{l'}(\mathbf{r}'_2) \int \frac{d^3 r'_1}{(2\pi)^{3/2}} e^{i\mathbf{p}_1 \cdot \mathbf{r}'_1} \psi_{l'}^*(\mathbf{r}'_1) \\ & = \int d^3 x e^{-i\mathbf{q} \cdot \mathbf{x}} \int \frac{d^3 \Delta x}{(2\pi)^3} e^{-i\mathbf{K} \cdot \Delta \mathbf{x}} \psi_l^*(\mathbf{x} + \frac{\Delta \mathbf{x}}{2}) \psi_l(\mathbf{x} - \frac{\Delta \mathbf{x}}{2}) \\ & \quad \times \int d^3 y e^{i\mathbf{q} \cdot \mathbf{y}} \int \frac{d^3 \Delta y}{(2\pi)^3} e^{i\mathbf{K} \cdot \Delta \mathbf{y}} \psi_{l'}^*(\mathbf{y} - \frac{\Delta \mathbf{y}}{2}) \psi_{l'}(\mathbf{y} + \frac{\Delta \mathbf{y}}{2}), \end{aligned} \quad (26)$$

where we have defined $\mathbf{K} = (\mathbf{p}_1 + \mathbf{p}_2)/2$ as the two- Q -boson average momentum, and $\mathbf{q} = \mathbf{p}_1 - \mathbf{p}_2$ as their relative momentum. For writing the last equality, we have also changed variables as follows: $\mathbf{r}_1 - \mathbf{r}_2 = \Delta \mathbf{x}$; $\mathbf{r}_1 + \mathbf{r}_2 = 2\mathbf{x}$; $\mathbf{r}'_1 - \mathbf{r}'_2 = \Delta \mathbf{y}$; $\mathbf{r}'_1 + \mathbf{r}'_2 = 2\mathbf{y}$.

Then we can define the Wigner function associated to the state l as

$$g_l(\mathbf{x}, \mathbf{K}) = \int \frac{d^3 \Delta x}{(2\pi)^3} e^{-i\mathbf{K} \cdot \Delta \mathbf{x}} \psi_l^*(\mathbf{x} + \frac{\Delta \mathbf{x}}{2}) \psi_l(\mathbf{x} - \frac{\Delta \mathbf{x}}{2}) . \quad (27)$$

We can proceed analogously to define the equivalent function for the integration in \mathbf{y} and $\Delta \mathbf{y}$, remembering that $g_l(\mathbf{x}, \mathbf{K}) = g_l^*(\mathbf{x}, \mathbf{K})$. Then, denoting by

$$g(\mathbf{x}, \mathbf{K}) = \sum_l N_l g_l,$$

we can finally define the generalized Wigner function of the problem as

$$\begin{aligned} g(\mathbf{x}, \mathbf{K}; \mathbf{y}, \mathbf{K}) &= g(\mathbf{x}, \mathbf{K}) g(\mathbf{y}, \mathbf{K}) - (1 - Q) \\ & \sum_l \left\{ N_l^2 \left[\frac{\exp(\frac{1}{T}(E_l - \mu)) + Q}{\exp(\frac{1}{T}(E_l - \mu)) - Q^2} \right] g_l(\mathbf{x}, \mathbf{K}) g_l(\mathbf{y}, \mathbf{K}) \right\} . \end{aligned} \quad (28)$$

We see that, for $Q = 1$, the above expression is reduced to the usual result of the original Wigner function, i.e., $g(\mathbf{x}, \mathbf{K}; \mathbf{y}, \mathbf{K}) = g(\mathbf{x}, \mathbf{K}) g(\mathbf{y}, \mathbf{K})$. On the other hand, for $Q = 0$, Eq. (28) is identically zero, as it should be in the limit of Boltzmann statistics.

By means of this Wigner function, the two- Q -boson correlation function can be rewritten as

$$C_2(\mathbf{p}_1, \mathbf{p}_2) = 1 + \frac{\iint e^{-i\mathbf{q} \cdot (\mathbf{x} - \mathbf{y})} g(\mathbf{x}, \mathbf{K}; \mathbf{y}, \mathbf{K}) d\mathbf{x} d\mathbf{y}}{\int g(\mathbf{x}, \mathbf{p}_1) d\mathbf{x} \int g(\mathbf{y}, \mathbf{p}_2) d\mathbf{y}} \quad (29)$$

The above generalized Wigner function, $g(\mathbf{x}, \mathbf{K})$, can be interpreted as the probability of finding a Q -boson at point \mathbf{x} with momentum \mathbf{K} . Differently from previous formulations we see that, if pions are treated as Q -bosons under certain regimes, there is now an additional term in Eq. (28). The modified two-particle Wigner function no longer can be reduced to the Fourier transform of the product of two single-particle Wigner functions, but acquires an extra factor depending on Q in a non-trivial way. As a consequence, for $0 \leq Q \leq 1$, we can anticipate that the correlation function would be narrower and the intercept, λ would drop below unity, to start with. We will illustrate more clearly the effects of the *deformation parameter*, Q , on the correlation function and on the chaoticity parameters in the next section, by means of two toy models.

In summary, we could say that, maybe under certain circumstances, pions produced in heavy-ion collisions could be treated as free particles. Nevertheless, and as motivated in the beginning of the present section, in many others, the interactions of pions among themselves and with other particles produced in relativistic heavy-ion collisions may not be negligible. In these cases, similarly to what has been suggested in Ref. [15,17], what it is proposed here is to mimic those interactions by considering pions as Q -bosons. In particular, the interpretation of Q as an effective parameter reflecting the fermionic constituentes [16] of the Q -bosons is appealing. Mainly if we consider that unconfined degrees of freedom could be produced in high energy heavy ion collisions and manifest themselves as Q -bosons in the pre-bosonic stages. In this sense, they would be regarded as *memory traces* from those pre-confined stages, just before the boson emission.

III. TWO- Q -BOSON CORRELATION FROM A FINITE VOLUME

A. Toy model

To explore the effects of the deformation parameter Q and of the boundary on the single- and two- Q -boson distribution functions, we assume that they are confined in a one-dimension box, $[0, L]$, for simplicity, since the three-dimensional extension should be straightforward. It can be easily checked that the corresponding wavefunction in the 1-D case is given by

$$\psi_k(x) = \sqrt{\frac{2}{L}} \sin k \cdot x, \quad (30)$$

with

$$k \cdot L = n\pi, n = 1, 2, 3, \dots \quad (31)$$

Then, the corresponding Fourier transform, $\tilde{\psi}_k(p)$, can be expressed as

$$\tilde{\psi}_k(p) = \frac{1}{(2\pi)^{1/2}} \frac{1}{\sqrt{2L}} \left[\frac{\exp(i(k-p)L) - 1}{p - k} - \frac{\exp(-i(k+p)L) - 1}{p + k} \right], \quad (32)$$

or, equivalently, its square modulus would be written as

$$|\tilde{\psi}_k(p)|^2 = \frac{1}{\pi L} \left[\frac{\sin^2 \frac{(p-k)L}{2}}{(p-k)^2} + \frac{\sin^2 \frac{(p+k)L}{2}}{(p+k)^2} + \frac{2 \sin(\frac{(k-p)L}{2}) 2 \sin(\frac{(k-p)L}{2})}{(p-k)(p+k)} \cos(kL) \right]. \quad (33)$$

On the other hand, if we recall the definition of the delta function

$$\delta(x) = \lim_{L \rightarrow \infty} \frac{1}{\pi} \frac{\sin(x \cdot L)}{x}, \quad (34)$$

it is easily verified that, when $L \rightarrow \infty$, we have

$$P_1(p) = \frac{L}{2\pi} N_p = \frac{L}{2\pi} \frac{1}{\exp(\frac{E_p - \mu}{T}) - Q}. \quad (35)$$

That is, in the limit of an infinit 1-D box, we obtain a modified Bose-Einstein distribution, where the deformation parameter Q replaces the unity factor, characteristic of BE statistics. In the finite box case, however, the spectrum should change more drastically, due to quantum effects, which we already showed in Ref. [6]. Moreover, in the present case, we will have both the finite size and the deformation parameter effects combined. To illustrate this, we show in Fig.1, the single spectrum distribution for two different box sizes. In that plot, as in all the others that will follow, we have chosen a null chemical potential, i.e., $\mu = 0$, for simplicity. For comparison, the corresponding modified Bose-Einstein spectrum distribution, given by Eq. (35), is also shown. It is interesting to note that for finite systems and decreasing values of the Q parameter, the width of single Q -boson distribution becomes broader, causing the maximum of the distribution to drop and the tail to rise, due to the conservation of the number of particles. The drop of the maximum for the same value of the momentum but for a smaller value of Q would correspond to a *weaker bosonic* behavior of the particles when compared to a $Q \rightarrow 1$, leading to a lower occupancy for small values of the momenta. The effect is more pronounced for increasing size of the emission region. On the other hand, decreasing the values of the deformation parameter Q has a similar effect as to decreasing the source emission size (see Ref. [6]), which is consistent with the uncertainty principle since, as the volume of the system decreases, the uncertainty in the pion coordinate decreases accordingly, causing a large fluctuation in the pion momentum distribution, which then becomes broader.

It is interesting to check how our result would compare with the interpretation given in Ref. [16], for which

Q could be viewed as an effective parameter reflecting the internal degrees of freedom of the bosons. In that reference, the deformation parameter Q is related to the ratio of the bosonic volume (L^3) to the system volume (V) by $Q \approx 1 - L^3/V$, where L is the boson's RMS radius. The ratio is then correlated to the degree of *bosonic overlap*. Although we do not consider here the bosons as extended objects, we still could try and see if that picture is compatible with our study. Let us first consider that the bosons have a fixed size. We compare then the above relation for two values of the system volume (where $V_2 > V_1$), associating a value of Q to each case. It is very simple to see that $Q_2 = \sqrt{1 - \frac{V_1}{V_2}(1 - Q_1^2)}$, i.e., an increase in the volume would result in a smaller deformation parameter, reflecting a smaller overlapping of the bosons and their constituents. In other words, for a fixed bosonic size and if we enlarge the volume that contains the bosons, the *resolution* decreases, implying that Q increases, i.e., gets closer to the boson statistics case for which $Q = 1$. Let us take another approach, by consering Q fixed and studying what happens for increasing volumes. In this case, a system of Q -bosons in a volume V_1 would be associted to a L_1^3/V_1 and another one, in similar conditions but with a volume $V_2 > V_1$, would have L_2^3/V_2 . In order to keep Q the same, the ratio had to be kept the same, which means that $L_2 > L_1$. This could be interpreted as if we could resolve better (i.e., higher resolution) the internal degrees of freedom in the second case (i.e., the boson with bigger L would be effectively be better probed regarding the its internal constituents). Consequently, for the same value of Q , we would expect that the larger the system is, more sensitive it would be to fixed value of Q . This is precisely what we can see in Fig.1, since the effect is more pronounced for $L = 8\text{fm}$ than it is for $L = 4\text{fm}$.

We have seen that the deformation parameter has a significant effect on the spectrum of the bosons. We discuss next what this implies to the interferometry of two-identical Q -bosons. In Fig. 2, the correlation functions for two values of the mean momentum K are shown for different deformed parameter, Q , as a function of the pair relative momentum, $|\mathbf{q}|$. For $Q = 1$, as already shown in Ref. [6], we see that, as the mean momentum increases, the source radius increases accordingly, due to the fact that contributions from small momenta come from smaller quantum l states which, in turn, corresponds to larger spread in coordinate space. Similar behavior in the radius is seen as Q decreases below unity. Another interesting point concerns the way the parameter Q changes the coherence parameter, λ , of the two- Q -boson correlation function. The effects on λ are more pronounced as smaller values of K are considered, which is natural, as for large values of the average momentum, the quantum effects become less relevant. From Eq.(25), we can see that, for increasing K , the dominant factors

come from the larger l states which, on the other hand, give smaller contribution to the two- Q -boson correlation, due to the factor N_λ , which decreases for increasing K , as can be seen from Eq. (9). Consequently, this makes the coherence parameter to vary more slowly with increasing values of K . This is illustrated in Fig. 3, where λ is shown as a function of Q for different values of the mean momentum and for different source radii. Again, we note that as the source radius becomes bigger, the Q effects on the coherent parameter becomes less significant, since in this case the quantum effects are smaller. In the plot, we only shown the variation of λ for Q in the interval $[0, 1]$, corresponding to $\lambda \leq 1$. Of course, if Q is larger than one, as one could expected from Eq.(25), the value of λ could be bigger than one. Also if the value of Q is negative, λ could be less than zero. However, we are treating here bosons with a modified commutation relation. Since no phenomena related to such an unexpected chaoticity was experimentaly observed yet for any type of bosons, we do not consider this case. In other words, our analysis refers basically to the above interval, $0 \leq Q \leq 1$. Nevertheless, we should keep in mind that the coherence parameter of the two identically charged Q -bosons could be bigger than one and less than zero, for some specific value of Q .

B. Q -bosons are confined inside a sphere

In this section, we consider the that the pions produced in high energy heavy-ion coolisions, treated here as the hypothetical Q -bosons, could be bounded in a sphere up to the time just preceding the system freezing-out. This is conceived in such a way that their distribution functions are essentially the ones they had while confined. Analogously to the procedure developped in [6], the pion wave function in this case should be determined by the solution of the Klein-Gordon equation, i.e.,

$$[\Delta + k^2] \psi(\mathbf{r}) = 0 , \quad (36)$$

where $k^2 = E^2 - m^2$ is the momentum of the pion. On writing the above equation, we have assumed confinement, i.e., the potential felt by the pion inside the sphere is zero, while outside it is infinite. The boundary condition to be respected by the solution is

$$\psi(\mathbf{r})|_{r=R} = 0 , \quad (37)$$

where R is the radius of the sphere at freeze-out time.

The normalized wave function corresponding to the solution of the above equation can easily be written as

$$\begin{aligned} \psi_{klm}(\mathbf{r}) &= \frac{1}{R J_{l+\frac{3}{2}}(kR)} \sqrt{\frac{2}{r}} Y_{lm}(\theta, \phi) J_{l+\frac{1}{2}}(kr) & (r < R), \\ &= 0 & (r \geq R). \end{aligned} \quad (38)$$

The momentum of the bounded particle, k , can be determined as the solution of the equation

$$J_{l+\frac{1}{2}}(kR) = 0 . \quad (39)$$

Inserting Eq. (38) into Eq. (7), we can determine the Fourier transform of the confined solution of a pion inside the sphere, as a function of the momentum \mathbf{p} , as [6]

$$\tilde{\psi}_{klm}(\mathbf{p}) = \sqrt{\frac{2}{p}} i^l Y_{lm}(\hat{p}) \left[\frac{-k}{p^2 - k^2} \right] J_{l+\frac{1}{2}}(pR) . \quad (40)$$

In terms of Eq. (19) and (20), the single-inclusive distribution function can be written as

$$\begin{aligned} P_1(\mathbf{p}) &= \sum_{klm} N_{klm} \tilde{\psi}_{klm}^*(\mathbf{p}) \tilde{\psi}_{klm}(\mathbf{p}) \\ &= \sum_{k,l} \frac{1}{\exp(\frac{E_{kl}-\mu}{T}) - Q} \left(\frac{2l+1}{2\pi p} \right) \left(\frac{k J_{l+\frac{1}{2}}(pR)}{p^2 - k^2} \right)^2 , \end{aligned} \quad (41)$$

In the limit $R \rightarrow \infty$, the single particle spectrum, can then written as

$$P_1(\mathbf{p}) = \frac{1}{\exp(\frac{E_p-\mu}{T}) - Q} \left[\frac{V}{(2\pi)^3} \right] , \quad (42)$$

where $V = \frac{4\pi}{3} R^3$ is the volume of the sphere. We see from Eq. (42) that the modified Bose Einstein distribution is recovered in the limit of a very large volume.

In Fig. 4, the normalized single-particle distribution is plotted as a function of $|\mathbf{p}|$. We clearly see that, due to the boundary effects, the maximum value of $|\mathbf{p}|$ in the spectrum decreases for decreasing volumes, being always smaller than the case corresponding to the $R \rightarrow \infty$ limit. This is, however, similar to the result obtained with the previous example of the 1-D box, and the confinement does not seem to cause a significant effect on the spectrum.

We can write the expectation value of the product of two Q -boson creation operators in momentum space as before, resulting in

$$\begin{aligned} \langle \hat{\psi}^\dagger(\mathbf{p}_1) \hat{\psi}(\mathbf{p}_2) \rangle &= \sum_{klm} \frac{\tilde{\psi}_{klm}^*(\mathbf{p}_1) \tilde{\psi}_{klm}(\mathbf{p}_2)}{\exp(\frac{E_{kl}-\mu}{T}) - Q} \\ &= \sum_{klm} \frac{1}{\exp(\frac{E_{kl}-\mu}{T}) - Q} \times \\ &\quad \sqrt{\frac{2}{p_1}} (-i)^l Y_{lm}^*(\hat{p}_1) \left[\frac{-k}{p_1^2 - k^2} \right] J_{l+\frac{1}{2}}(p_1 R) \\ &\quad \sqrt{\frac{2}{p_2}} (i)^l Y_{lm}^*(\hat{p}_2) \left[\frac{-k}{p_2^2 - k^2} \right] J_{l+\frac{1}{2}}(p_2 R) \\ &= \sum_{kl} \frac{1}{\exp(\frac{E_{kl}-\mu}{T}) - Q} \sqrt{\frac{4}{p_1 p_2}} \end{aligned}$$

$$\begin{aligned} &\frac{k^2}{(p_1^2 - k^2)(p_2^2 - k^2)} J_{l+\frac{1}{2}}(p_1 R) \\ &J_{l+\frac{1}{2}}(p_2 R) \left(\frac{2l+1}{4\pi} \right) P_l(\hat{p}_1 \cdot \hat{p}_2) . \end{aligned} \quad (43)$$

The two-pion interferometry correlation function can then be estimated by inserting the above expressions (41) and (43), into Eq. (23). We see from the above results that, in general, this function depends on the angle between \mathbf{p}_1 and \mathbf{p}_2 , similarly to what was discussed in [6]. For the sake of simplicity, however, we will also consider here \mathbf{p}_1 parallel to \mathbf{p}_2 , implying that $P_l(\hat{p}_1 \cdot \hat{p}_2 = \pm 1) = (\pm 1)^l$. The results for two-pion interferometry corresponding to two different values of the pair average momentum $\mathbf{K} = (\mathbf{p}_1 + \mathbf{p}_2)/2$ but fixed temperature are shown in Fig. 5. For $Q = 1$ we can see that, as the pair average momentum, K , increases, the apparent source radius becomes bigger, which reproduces the result obtained in Ref. [6]. However, considering $K = 0.3$ GeV/c, if we compare the cases corresponding to $Q = 1$ and $Q = 0.5$, respectively, we see that the resulting correlation function becomes narrower and the intercept, λ , drops below its previous unit value. On the other hand, if we now keep this value of $Q = 0.5$ but consider $K = 0.5$ GeV/c, the width is still narrower, however, the intercept is higher than that corresponding to $K = 0.3$ GeV/c, but still below two. This due to the fact that for smaller momentum pairs, the quantum effects are stronger, as in the previous toy model studied in Fig. 2, and it comes from the contribution of the third term in two- Q -boson interferometry formula, in Eq.(29). Similar to Fig. 3, we plot λ vs. Q for different momentum values and source radii, in Fig.6. Once again we see the similarity with the corresponding result of the previous example, in Fig. 3: λ becomes bigger as either the total momentum increases or the source radii increases. In summary, by comparing the correlation corresponding to the two toy models, we see that the general behavior is roughly reproduced in both, suggesting that the confinement of the Q -bosons do not seem to play an important role in their interferometric relation. Nevertheless, the effects for the bounded case are less pronounced as compared to the unbounded one, at least for the set of parameters adopted in the calculation.

We could understand these results by noting that pions with larger momentum come from larger quantum l states which, in turn, correspond to a smaller spread in coordinate space. Due to the weight factor in Eq. (23), of modified Bose-Einstein form, larger quantum states will give a smaller contribution to the source distribution, causing the effective source radius to appear larger. On the other hand, this behavior is interesting if we compare to results corresponding to expanding systems. In this last case, the probed part of the system decreases with increasing average momentum [21,22]. Naturally, our present approach does not consider the effects of ex-

pansion and the enlargement of the system's apparent dimensions with increasing K , seen in Figure 5, has its origin in the strong sensitivity to the dynamical matrix. In Ref. [23], the combined effects of a finite boundary and an expanding system were considered together. What they observed was an opposite effect, i.e., the effective source radius extracted from two-pion interferometry would decrease as K increases. However, for small values of the momentum K , it seems that the boundary effects are dominant over the expansion effects.

In Fig. 6, we plot the chaoticity parameter λ vs. Q for different momenta and source radii. The similarity to the results in Fig. 3 is evident. The intercept becomes much smaller than two for decreasing values of the total momentum, K , or for increasing values of the source radius. The intercept will progressively decrease if the total momentum becomes smaller, or, alternatively, if the source size increases, as expected since the quantum effects are more prominent for smaller momenta. Again, the comments relating these results to the speculation in Ref. [16] apply here, as in the previous example.

IV. CONCLUSIONS

In this paper, we derive spectrum and correlation function relations by adopting the density matrix given in Eq.(10), suitable for describing charged Q -bosons. The finite volume effects on the Q -boson spectrum were then studied in Figures 1 and 4, for two specific examples, leading to similar results as in Ref. [8,10,11], for $Q = 1$. We find that the small momentum region is depleted for the modified Bose-Einstein distribution with respect to case when $Q \rightarrow 1$. The effects on two equally charged Q -boson correlation function were also analyzed here. The results in Figures 2 and 5 show that the correlation function shrinks for increasing average pair momentum, corresponding to an increase of its inverse width [6]. We also observe that its intercept drops for decreasing Q . In other words, it was shown in Figures 3 and 6 that the coherence parameter, λ , decreases for increasing Q , for the same values of the average transverse momentum and source radius. On the other hand, λ becomes larger when either the mean momentum of two- Q -boson or the source radius increases. This result reflects a strong sensitivity to the dynamical matrix, through the modified Bose-Einstein weight factor. For $Q = 1$, previous pion interferometry results are regained. We have also derived a generalized version of the two-boson Wigner function, extended to allow for treating the case of two Q -bosons. This generalization, however, is reduced to its well-known form in the limit $Q \rightarrow 1$, as it should.

We also analysed in the current work how our results compare with the interpretation given in Ref. [16], for which Q could be viewed as an effective parameter reflecting the internal degrees of freedom of the bosons.

We saw that, if we consider a fixed value for the deformation parameter, Q , and compare results for increasing volumes, we see that our result would be compatible with that interpretation. To summarize the comparison we could say that, for increasing volumes and keeping the same value of Q , we would have to increase the *resolution*, i.e., the sensitivity of the probe to the internal degrees of freedom of the boson. Consequently, for the same value of Q , we would expect that the larger the system is, more sensitive it would be to this parameter. This is precisely what we can see in Fig.1, since the effect is more pronounced for $L = 8\text{fm}$ than it is for $L = 4\text{fm}$.

The derivation analysed here has several common features with the one in Ref. [15,17] but here we adopt a entirely different approach, focussing in what seems to us the most important part of an interferometric analysis, i.e., the correlation functions themselves. We also analyse the effects in the spectra and in the chaoticity parameter but, again, our result is more general than in that reference, since it is there restricted to single modes.

Another remark concerns the relation of the parameter λ and its possible interpretation as a partial coherence of the emitting source for values below unity. It is well-known that many effects, such as resonances, dynamical and multiparticle effects, as well as kinematical cuts, could also contribute to yield values of λ smaller than the unity, and compete with the effects caused by decreasing values of Q shown here. For this reason and for keeping the analysis simple, not taking these effects into account, we prefer not to compare with experimental data.

Also, for completeness, we derive in the Appendix, the spectrum and the correlation function associated to the so-called *type-B Q -boson interferometry*, in Ref [15], corresponding to slightly different commutation relations. The derived relations are in Eq.(45,48), Eq.(46,49), respectively. Also for this case, we propose a generalized form for the Wigner function, as can be seen in Eq.(50).

ACKNOWLEDGMENTS

S.S.P. is deeply grateful to Larry McLerran and the Nuclear Theory Group at BNL, as well as to Keith Ellis and the Theoretical Physics Department at Fermilab, for their kind hospitality when finalizing this work. This research was partially supported by CNPq (Proc. N. 200410/82-2). This manuscript has been authored under Contracts No. DE-AC02-98CH10886 and No. DE-AC02-76CH0300 with the U.S. Department of Energy. This work was also partially supported by Fundação de Amparo à Pesquisa do Estado de São Paulo (FAPESP, Proc. N. 1998/05340-2 and 1998/2249-4), Brazil, and NSERC of Canada.

- [1] See for example: C.Y. Wong, *Introduction to high energy heavy-ion collisions*, (World Scientific, Singapore, 1994); *Quark-Gluon-Plasma 2*, edited by R.C. Hwa (World Scientific, Singapore, 1995).
- [2] Proceedings of Quark Matter 2001, ...
- [3] R. Hanbury-Brown and R.Q. Twiss, *Phil. Mag.* **45**, 663 (1954); *Nature* **177**, 27 (1956) and **178**, 1447 (1956).
- [4] G. Goldhaber, S. Goldhaber, W. Lee, and A. Pais, *Phys. Rev.* **120**, 300 (1960).
- [5] for a long list of references on interferometry, see i) W.A. Zajc, *Il Ciocco 1992, Particle production in highly excited matter* (NATO Advanced Study Institute), p. 435, Castelvecchio Pascoli, Italy, 12-24 Jul 1992; ii) D. H. Boal, C. K. Gelbke, and B. K. Jennings, *Rev. Mod. Phys.* **62**, 553 (1990); iii) R. M. Weiner, *Bose-Einstein Correlation in Particle and Nuclear Physics*, J. Wiley & Sons (1997); iv) U. Heinz and B. V. Jacak, *Ann. Rev. Nucl. Part. Sci.* **49**, 529 (1999).
- [6] Q. H. Zhang and S. Padula, *Phys. Rev. C* **62** 024902 (2000).
- [7] E. V. Shuryak, *Phys. Rev. D* **42**, 1764 (1990).
- [8] C.Y. Wong, *Phys. Rev. C* **43**, 902 (1993).
- [9] Yu. Sinyukov, *Nucl. Phys.* **A566**, 589c (1994).
- [10] M. Mostafa and C.Y. Wong, *Phys. Rev. C* **51**, 2135 (1995).
- [11] A. Ayala and A. Smerzi, *Phys. Lett.* **B405**, 20 (1997); A. Ayala, J. Barreiro and L. M. Montaño, *Phys. Rev. C* **60**, 014904 (1999).
- [12] S. Sarkar, P. K. Roy, D. K. Srivastava, and B. Sinha, *J. Phys.* **G22**, 951 (1996).
- [13] O.W. Greenberg, *Phys. Rev. Lett.* **64**, 705 (1990), and *Phys. Rev. D* **43**, 4111 (1991).
- [14] D.D. Coon, S. Yu and M. Baker, *Phys. Rev. D* **5**, 1429 (1972); P. Kulish and E. Damaskinsky, *J. Phys. A* **23**, L 415 (1990); S. Chaturvedi, A. K. Kapoor, R. Sandhya, V. Srinivasan and R. Simon, *Phys. Rev. A* **43**, 4555 (1991).
- [15] D. V. Anchishkin, A. M. Gavrilik and N. Z. Iorgov, *Eur. Phys. J. A* **7** 229 (2000).
- [16] S. S. Avancini and G. Krein, *J. Phys. A: Math. Gen.* **28**, 685 (1995).
- [17] D. V. Anchishkin, A. M. Gavrilik and S. Y. Panitkin, *hep-ph/0112262*.
- [18] S. Pratt, *Phys. Rev. Lett.* **53**, 1219 (1984).
- [19] S. S. Padula, M. Gyulassy, and S. Gavin, *Nucl. Phys. B* **329**, 357 (1990).
- [20] W. Q. Chao, C. S. Gao and Q. H. Zhang; *Phys. Rev. C* **49**, 3224 (1994).
- [21] Urs. Wiedemann and U. Heinz, *Phys. Rept.* **318**, 145 (1999).
- [22] T. Csorgo, *hep-ph/0001233*.
- [23] A. Ayala and A. Sanchez, *Phys. Rev. C* **63**, 064901 (2001).

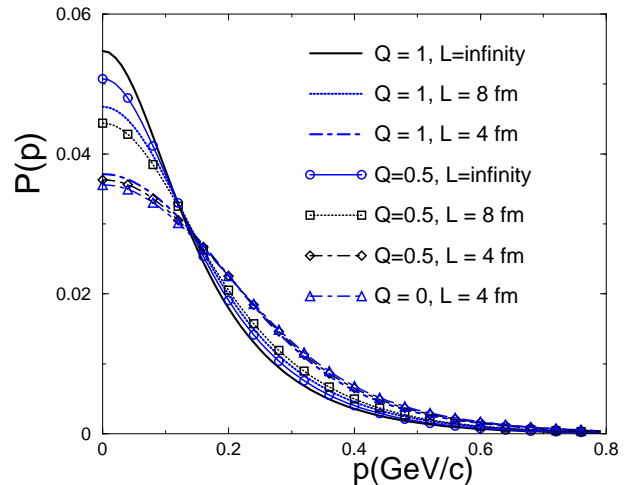


FIG. 1. Normalized spectrum (in arbitrary units) vs. momentum $|p|$ (in GeV/c). The input temperature is $T = 0.14 \text{ GeV}$ and the chemical potential is $\mu = 0$. The solid line corresponds to the modified Bose-Einstein distribution, i.e., to the limit $R \rightarrow \infty$. The dotted and dashed lines correspond, respectively, to the $L = 8 \text{ fm}$ and $L = 4 \text{ fm}$ cases. The wider line corresponds to the case of $Q = 0.5$ and the thinner one corresponds to $Q = 1$.

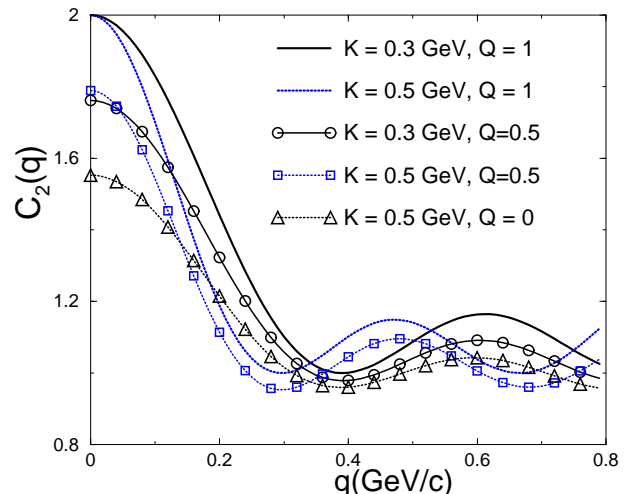


FIG. 2. Two-pion correlation vs. momentum difference $|\mathbf{q}|$ (in GeV/c). The input temperature is $T = 0.14 \text{ GeV}$ and the chemical potential is $\mu = 0$. The solid line corresponds to the case mean momentum $K = 0.2 \text{ GeV}$ and dashed line corresponds to the case $K = 0.3 \text{ GeV}$. The wider line corresponds to the case of $Q = 0.5$ and the thinner one corresponds to $Q = 1$. The box size is $L = 4 \text{ fm}$.

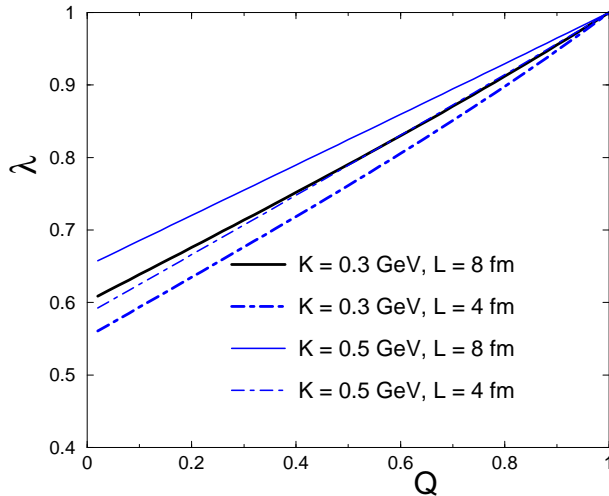


FIG. 3. coherent parameter vs. parameter Q . The input temperature is $T = 0.14$ GeV and the chemical potential is $\mu = 0$. The solid line corresponds to the case mean momentum $K = 0.1$ GeV and dashed line corresponds to the case $K = 0.3$ GeV. The wider line corresponds to the case of $L = 8$ fm and the thinner one corresponds to $L = 4$ fm.

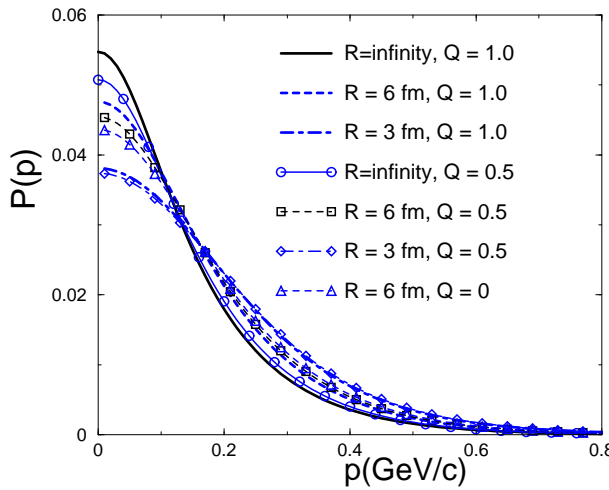


FIG. 4. $P(p)$ vs. p . The input temperature is $T = 0.12$ GeV and the chemical potential is $\mu = 0$. The solid line corresponds to the case $R = 3$ fm. The dotted-line corresponds to the case $R = 6$ fm. The dashed line corresponds to the case, $R = \infty$. The wider line corresponds to the case of $Q = 0.5$ and the thinner one corresponds to $Q = 1$.

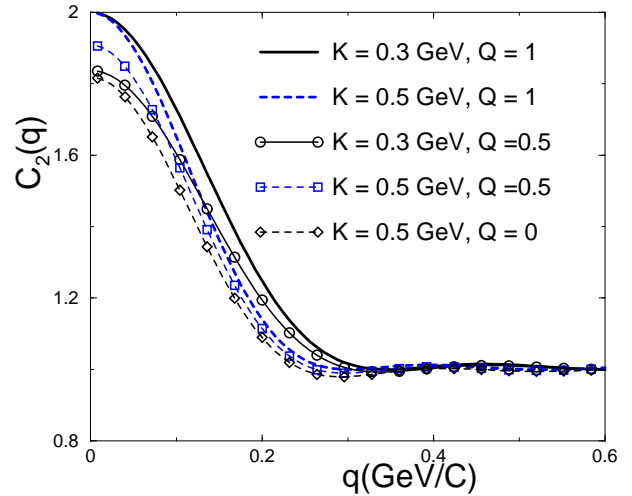


FIG. 5. Two-pion correlation vs. momentum difference $|\mathbf{q}|$ (in GeV/c). The input temperature is $T = 0.12$ GeV and the chemical potential is $\mu = 0$. The solid line corresponds to the case mean momentum $K = 0.3$ GeV and dashed line corresponds to the case $K = 0.5$ GeV. The wider line corresponds to the case of $Q = 0.5$ and the thinner one corresponds to $Q = 1$. The sphere size is $R = 3$ fm.

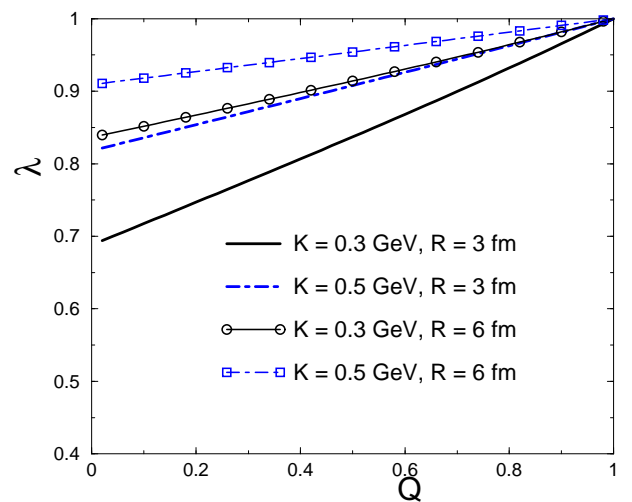


FIG. 6. coherent parameter vs. parameter Q . The input temperature is $T = 0.12$ GeV and the chemical potential is $\mu = 0$. The solid line corresponds to the case mean momentum $K = 0.1$ GeV and dashed line corresponds to the case $K = 0.3$ GeV. The wider line corresponds to the case of $R = 5$ fm and the thinner one corresponds to $R = 3$ fm.

APPENDIX

For completeness, we will also derive below the so-called type-B qboson interferometry formulation, as defined in Ref. [15]. For type-B Q -boson, the operators b_i and b_j satisfy the following commutation relations

$$\begin{aligned} b_l b_{l'}^\dagger - Q^{\delta_{l,l'}} b_{l'}^\dagger b_l &= \delta_{l,l'} Q^{-N_l} \\ b_l b_{l'}^\dagger - Q^{-\delta_{l,l'}} b_{l'}^\dagger b_l &= \delta_{l,l'} Q^{N_l} \\ [b_l, b_{l'}] &= [b_l^\dagger, b_{l'}^\dagger] = 0, \\ [\hat{N}_l, b_{l'}] &= -\delta_{l,l'} b_l \\ [\hat{N}_l, b_{l'}^\dagger] &= \delta_{l,l'} b_l^\dagger, \\ [\hat{N}_l, \hat{N}_{l'}] &= 0. \end{aligned} \quad (44)$$

In the above relations Q is a parameter, which can be assumed within $[-1, 1]$. If we define it, following Ref. [15], as $Q = e^{i\theta}$ ($0 \leq \theta < 2\pi$) or, equivalently, $\cos(\theta) = \frac{1}{2}(Q + Q^{-1})$, then

$$\begin{aligned} \langle b_l^\dagger b_l \rangle &= \\ &= \frac{\exp(\frac{1}{T}(E_l - \mu)) - 1}{\exp(\frac{2}{T}(E_l - \mu)) - 2 \cos(\theta) \exp(\frac{1}{T}(E_l - \mu)) + 1} = \\ &= \frac{\exp[\frac{-1}{2T}(E_l - \mu)] \sinh[\frac{1}{2T}(E_l - \mu)]}{\cosh[\frac{1}{T}(E_l - \mu)] - \cos(\theta)} \end{aligned} \quad (45)$$

and

$$\begin{aligned} \langle b_l^\dagger b_l^\dagger b_l b_l \rangle &= \\ &= \frac{2 \cos(\theta)}{\exp(\frac{2}{T}(E_l - \mu)) - 2 \cos(2\theta) \exp(\frac{1}{T}(E_l - \mu)) + 1} \\ &= \frac{\cos(\theta) \exp[\frac{-1}{T}(E_l - \mu)]}{\cosh[\frac{1}{T}(E_l - \mu)] - \cos(2\theta)}. \end{aligned} \quad (46)$$

As before, the expectation value $\langle \hat{b}_l^\dagger \hat{b}_{l'} \rangle$ is related to the occupation probability of the single-particle state l , $N_l^{(b)}$, by a similar relation, i.e.,

$$\langle \hat{b}_l^\dagger \hat{b}_{l'} \rangle = \delta_{l,l'} N_l^{(b)}. \quad (47)$$

Then similar to the derivation of Eq.(16) and Eq.(20), we have

$$P_1(\mathbf{p}) = \sum_l \langle b_l^\dagger b_l \rangle \tilde{\psi}_l^*(\mathbf{p}) \tilde{\psi}_l(\mathbf{p}) \quad (48)$$

and

$$\begin{aligned} P_2(\mathbf{p}_1, \mathbf{p}_2) &= P_1(\mathbf{p}_1) P_1(\mathbf{p}_2) + \left| \sum_l \tilde{\psi}_l^*(\mathbf{p}_1) \tilde{\psi}_l(\mathbf{p}_2) \right|^2 \\ &+ \sum_l \tilde{\psi}_l^*(\mathbf{p}_1) \tilde{\psi}_l^*(\mathbf{p}_2) \tilde{\psi}_l(\mathbf{p}_1) \tilde{\psi}_l(\mathbf{p}_2) [\langle b_l^\dagger b_l^\dagger b_l b_l \rangle - 2 \langle b_l^\dagger b_l \rangle] \end{aligned}$$

$$\begin{aligned} &= P_1(\mathbf{p}_1) P_1(\mathbf{p}_2) + \sum_{l,l'} N_l N_{l'} \tilde{\psi}_l^*(\mathbf{p}_1) \tilde{\psi}_{l'}^*(\mathbf{p}_2) \tilde{\psi}_l(\mathbf{p}_2) \tilde{\psi}_{l'}(\mathbf{p}_1) \\ &\quad \left\{ 1 - \delta_{l,l'} (1 - \cos \theta) \left[\frac{4 \cosh^2(\frac{E_l - \mu}{2T}) + \frac{\cos \theta (\cos \theta - 1)}{\sinh^2(\frac{E_l - \mu}{2T})}}{\cosh(\frac{E_l - \mu}{T}) - \cos(2\theta)} \right] \right\}. \end{aligned} \quad (49)$$

Analogously to what was done at the end of Section II, we can also define a modified Wigner function for type-B Q -boson. The new Wigner function for this case can be defined similarly as before, resulting in

$$\begin{aligned} g^{(b)}(\mathbf{x}, \mathbf{K}; \mathbf{y}, \mathbf{K}) &= g^{(b)}(\mathbf{x}, \mathbf{K}) g^{(b)}(\mathbf{y}, \mathbf{K}) - \\ &\quad \sum_l \left\{ (N_l^{(b)})^2 (1 - \cos \theta) \left[\frac{4 \cosh^2(\frac{E_l - \mu}{2T}) + \frac{\cos \theta (\cos \theta - 1)}{\sinh^2(\frac{E_l - \mu}{2T})}}{\cosh(\frac{E_l - \mu}{T}) - \cos(2\theta)} \right] \right\} \end{aligned} \quad (50)$$

Then the two-pion interferometry formula follows analogously to Eq.(29) for this case, i.e.,

$$C_2^{(b)}(\mathbf{p}_1, \mathbf{p}_2) = 1 + \frac{\int \int e^{-i\mathbf{q} \cdot (\mathbf{x} - \mathbf{y})} g^{(b)}(\mathbf{x}, \mathbf{K}; \mathbf{y}, \mathbf{K}) d\mathbf{x} d\mathbf{y}}{\int g^{(b)}(\mathbf{x}, \mathbf{p}_1) d\mathbf{x} \int g^{(b)}(\mathbf{y}, \mathbf{p}_2) d\mathbf{y}} \quad (51)$$